

Inter-comparison of online and offline methods for measuring ambient heavy and trace elements and water-soluble inorganic ions (NO_3^- , SO_4^{2-} , NH_4^+ and Cl^-) in $\text{PM}_{2.5}$ over a heavily polluted megacity, Delhi

Himadri Sekhar Bhowmik¹, Ashutosh Shukla¹, Vipul Lalchandani¹, Jay Dave², Neeraj Rastogi², Mayank Kumar³, Vikram Singh⁴, and Sachchida Nand Tripathi^{1*}

¹ Department of Civil Engineering, Indian Institute of Technology Kanpur, Kanpur, India

^{1*} Department of Civil Engineering and Centre for Environmental Science and Engineering, Indian Institute of Technology Kanpur, Kanpur, India

² Geosciences Division, Physical Research Laboratory, Ahmedabad, India

³ Department of Mechanical Engineering, Indian Institute of Technology Delhi, New Delhi, India

⁴ Department of Chemical Engineering, Indian Institute of Technology Delhi, New Delhi, India

Correspondence to: S. N. Tripathi (snt@iitk.ac.in)

Keywords: Aerosol mass spectrometer (AMS), Xact 625i ambient metal mass monitor, Ion Chromatography (IC), ICP-MS, elemental composition.

Abstract

Characterizing the chemical composition of ambient particulate matter (PM) provides valuable information on the concentration of secondary species, toxic metals and assists in the validation of abatement techniques. The chemical components of PM can be measured by sampling on filters and analysing them in the laboratory or using real-time measurements of the species. It is important for the accuracy of the PM monitoring networks that measurements from the offline and online methods are comparable and biases are known. The concentrations of water-soluble inorganic ions (NO_3^- , SO_4^{2-} , NH_4^+ and Cl^-) in $\text{PM}_{2.5}$ measured from the 24 hrs filter samples using ion chromatography (IC) were compared with the online measurements of inorganics from aerosol mass spectrometer (AMS) with a frequency of 2 mins. Also, the concentrations of heavy and trace elements determined from the 24 hrs filter samples using inductively coupled plasma mass spectroscopy (ICP-MS) were compared with the online measurements of half-hourly heavy and trace metal's concentrations from Xact 625i ambient metal mass monitor. The comparison was performed over two seasons (summer and winter) and at two sites (Indian Institute of Technology, Delhi and Indian Institute of Tropical Meteorology, Delhi) which are located in

Delhi, NCR, India, one of the heavily polluted urban areas in the world. Collocated deployments of the instruments helped to quantify the differences between online and offline measurements and evaluate the possible reasons for positive and negative biases. The slopes for SO_4^{2-} and NH_4^+ were closer to 1:1 line during winter and decreased during summer at both sites. The higher concentrations on the filters were due to the formation of particulate $(\text{NH}_4)_2\text{SO}_4$. Filter-based NO_3^- measurements were lower than online NO_3^- during summer at IITD and winter at IITMD due to the volatile nature of NO_3^- from the filter substrate. Offline measured Cl^- was consistently higher than AMS derived Cl^- during summer and winter at both sites. Based on their comparability characteristics, elements were grouped under 3 categories. The online element data were highly correlated ($R^2 > 0.8$) with the offline measurements for Al, K, Ca, Ti, Zn, Mn, Fe, Ba, and Pb during summer at IITD and winter at both the sites. The higher correlation coefficient demonstrated the precision of the measurements of these elements by both Xact 625i and ICP-MS. Some of these elements showed higher Xact 625i elemental concentrations than ICP-MS measurements by an average of 10-40% depending on the season and site. The reasons for the differences in the concentration of the elements could be the distance between two inlets for the two methods, line interference between two elements in Xact measurements, sampling strategy, variable concentrations of elements in blank filters and digestion protocol for ICP measurements.

1. Introduction

The adverse effect of ambient particulate matter (PM) on human health and the role of PM in visibility degradation, altering earth's radiation balance, and climate change has received global attention in the last two decades (Pope et al., 2009; Hong et al., 2019; Wang et al., 2019). To gain better insight into their properties, the chemical characterization of particulate matter and its source attribution is crucial. The National Capital Region (NCR), which includes India's capital (New Delhi) along with some districts (Gurugram, Faridabad, and Noida) of the adjoining states of Haryana, Rajasthan, and Uttar Pradesh, is one of the most polluted urban areas in northern India with a population over 47 million (Bhowmik et al., 2021). According to World Economic Forum, New Delhi was listed as the most polluted city globally, with an annual average $\text{PM}_{2.5}$ concentration of $\sim 140 \mu\text{g m}^{-3}$ (World Health Organisation, 2018). NCR has been a specific area for researchers for the past couple of years due to its unprecedented $\text{PM}_{2.5}$ levels. Various large and small scale industries, power plants, construction activities, and rapid increase in the vehicle numbers (11 million in 2018) (Rai et al., 2020) are among the several causes that massively reduces the air quality index (AQI) (Rai et al., 2020; Sharma & Kulshrestha, 2014). Further, the crop residue burning during the month of Oct-Nov in the adjoining states of Haryana and Punjab on a larger scale worsens the air quality.

For decades, the mass concentrations of major water soluble inorganic ions (WSIS) and heavy and trace metals in PM have been carried out by sampling them on filters and subsequently analysing them in laboratory. Water-soluble inorganic ions (WSIS) and heavy and trace elements from these filter samples are analyzed using ion chromatography (IC) (Bhowmik et al., 2021; Rengarajan et al., 2007; Rastogi & Sarin, 2005) and inductively coupled plasma-mass spectroscopy (ICP-MS) or inductively coupled plasma-optical emission spectroscopy (ICP-OES) (Patel et al., 2021) respectively. Usually, these filters are collected over 24 hrs interval. Traditional receptor models usually use these offline measured data of very low temporal resolution, making it challenging to characterize the short pollution episodes and dynamics of pollution sources. Further, un-denuded filter sampling can have both negative and positive artifacts due to volatile species (Lipfert, 1994; Pathak & Chan, 2005). The absorption of acidic and alkaline gases on the filter substrates, if not removed prior to sampling, can give positive artifacts and result in overestimating species concentration. Likewise, the evaporation of semi-volatile compounds (ammonium nitrate) from filter substrates can give negative biases and result in underestimating aerosol concentration and its species (Pathak & Chan, 2005; X. Zhang & McMurry, 1992). The degree of artifacts can be affected by several factors, including temperature, relative humidity, type of filter substrate, the aerosol loading on the filter substrate, etc. Transient events can also lead to mismatch. To overcome the limitations of low temporal resolution and avoid the artifacts associated with offline filter sampling, methods have been developed for measuring aerosol chemical composition at a higher time resolution in the order of hours or minutes.

Aerosol Mass Spectrometer (AMS) (Canagratna et al., 2007; Jayne et al., 2000; Jimenez et al., 2003) is one kind of such instrument, which provides size-resolved chemical composition of non-refractory submicron aerosols, e.g., organics, sulphate, nitrate, ammonium, and chloride at the order of hours or even minutes. For other important components, such as calcium (main constituents of soil dust and construction activities) and potassium (tracer of biomass burning), which AMS cannot measure, Xact ambient metal mass monitor can be used. It is capable of measuring 45 elements, e.g., Al, Si, P, S, Cl, K, Ca, Ti, V, Cr, Mn, Fe, Co, Ni, Cu, Zn, Ga, Ge, As, Se, Br, Rb, Sr, Y, Zr, Nb, Mo, Pd, Ag, Cd, In, Sn, Sb, Te, I, Cs, Ba, La, Ce, Pt, Au, Hg, Tl, Pb and Bi with a frequency of every 30 mins to 4 hours. However, the high time-resolution instruments measure lower range of species concentrations with higher limit of detection (LOD) than the offline based methods (Tremper et al., 2018). Both offline and online methods have their own strength and weaknesses. Uncertainties in offline filter analysis methods have been extensively studied (Pathak & Chan, 2005; Viana et al., 2006), but the novel online methods pose new problems (Wu & Wang, 2007). For example, when the ambient concentrations are very low, online measurements are often close to the MDL values due to the short integration times (Malaguti et al., 2015).

Previous studies in Delhi-NCR have used low time resolution filter-based methods for chemical characterization of submicron aerosols (Bhowmik et al., 2020; Nagar et al., 2017; Pant et al., 2015; S. K. Sharma et al., 2016; Singhai et al., 2017). On the other hand, there are only a few studies in Delhi-NCR that used high time resolution methods (HR-ToF-AMS, Q-ACSM, Xact) for characterization and source apportionment of coarse and fine particulate matters (Gani et al., 2019; Lalchandani et al., 2021; Rai et al., 2020, 2021; Singh et al., 2021; Tobler et al., 2020). Online and offline measurements both have their advantages and limitations. For both these measurements, the quality of the data highly depends on the calibration of the instruments. For Xact, the multi-element mix standard might not represent ambient elemental mix if the ambient particulate matters are too low or too high in concentration, affecting the collection properties of the filter (Indresand et al., 2013). For filter-based water-soluble inorganic ion and metal analysis, confidence in the data depends on the calibration as well as the volatility, solubility, and digestion protocol used for the extraction of water-soluble inorganic ions and elements, respectively. Thus, it is vital for monitoring networks that both the offline and online measurement methods give comparable results. Few published studies have compared inorganics and elements from filter-based measurements and semi-continuous methods (e.g., Furger et al., 2017; Nie et al., 2010). The inter-comparison in these studies is unjustified for highly polluted areas, as the specie values observed in these studies are much below MDL due to very low ambient concentration of secondary species and elements. It will be interesting to study the inter-comparison in highly polluted areas. To the best of our knowledge, there are neither any published seasonal and temporal comparisons of inorganics from high time resolution AMS measurements and filter-based measurements from ion chromatography nor any comparisons of heavy and trace metals from high time resolution Xact 625 ambient metal mass monitor and offline measurements from ICP-MS in the heavily polluted Delhi NCR region.

This study demonstrates a comparison between online and offline measurements of WSIS and heavy and trace metals at two sites in Delhi NCR during summer (June-July 2019), characterized by moderate levels of local pollution and winter (October-December 2019), affected by high levels of pollution from local sources and regional transport of crop residue burning emissions from adjoining state of Haryana and Punjab.

2. Methodology

2.1. Sampling sites

Delhi-NCR, a highly polluted urban area with an annual average PM_{2.5} concentration of 140 µg m⁻³ and a population of over 47 million, is surrounded by the Thar desert on its west and Indo-Gangetic Plain on its

east to south-east. The temperature is about $\sim 35^{\circ}\text{C}$ - 48°C during summer (April-June), and winter (December-February) is relatively cooler, with temperature ranges from $\sim 2^{\circ}\text{C}$ - 15°C (Bhowmik et al., 2020; Vipul Lalchandani et al., 2021; Tobler et al., 2020). The wind is mostly north-westerly during both summer and winter.

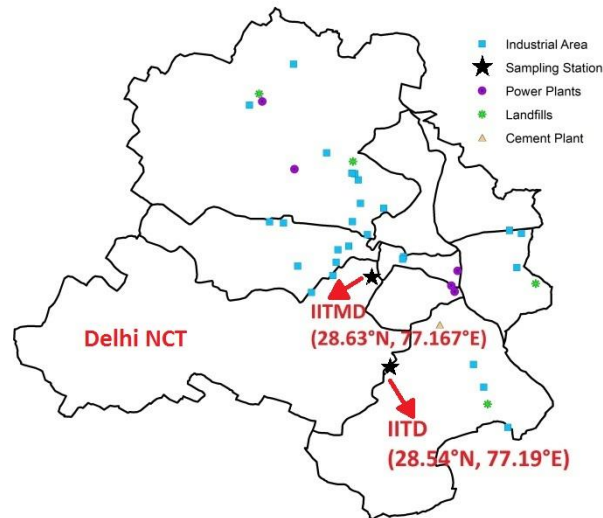


Fig.1. Sampling sites with various emission sources like power plants, industries, landfills, etc.

2.1.1. Delhi NCR site 1: IITD

High volume $\text{PM}_{2.5}$ samples were collected on the rooftop of the Centre for Atmospheric Science (CAS) building at the Indian Institute of Technology, Delhi (IITD) (28.54°N , 77.19°E ; ~ 218 m amsl) about ~ 15 m above the ground level. Further, one HR-ToF-AMS and Xact ambient metal mass monitor were deployed inside a temperature-controlled laboratory on the 3rd floor of the same building about ~ 10 m above the ground level. It is an educational institute as well as residential campus having restaurants nearby and very close to (< 200 m) heavy traffic road. Lalchandani et al., (2021); Rai et al., (2020) observed source signatures of emissions from industries, power plants, vehicles, and waste burning in this site.

2.1.2. Delhi NCR site 2: IITMD.

Offline $\text{PM}_{2.5}$ sampling was carried out on the rooftop of the main building at the Indian Institute of Tropical Meteorology Delhi (IITMD) (28.63°N , 77.167°E ; ~ 220 m above msl) about 15 m above the ground level. Moreover, HR-ToF-AMS and Xact ambient metal mass monitor were installed inside a

temperature-controlled laboratory on the 2nd floor of the same building at the height of ~8 m from the ground level. This site is placed in the central urban area of Delhi and surrounded by Central Ridge reserve forest and residential areas (Tobler et al., 2020) and around 14 km away in North West direction from IITD. A recent study by Lalchandani et al. (2021) observed the site is dominated by emissions from traffic, solid fuel burning, and oxidized organic aerosols. The location of the sampling sites are shown in Fig. 1.

2.2. Sampling details

2.2.1 Offline sampling

Biweekly 24 hrs (January-May and August-September 2019) and daily 24 h (June-July and October-December 2019) PM_{2.5} samples were collected on quartz filter substrates (Whatman; 8 × 12 inches) using a high-volume sampler (HVS) with a flow rate of 1.13 m³/min. Blanks were collected in the field by placing a fresh filter in the sampler while not running. A total of 64 filters (60 from IITD site during June-July 2019 including 4 blanks) were collected in summer whereas, a total of 186 filters (90 from each site during October-December 2019 plus 6 blanks) were collected in winter. The collected filters, including field blanks, were zip-locked and stored in the freezer at each site and periodically transported to CESE (Centre for Environmental Science and Engineering), IIT Kanpur, where they were further stored at -20°C in a deep freezer prior to analysis. For this study, the samples from the common period of offline and online sampling (October-December 2019) from the two sites were analyzed for WSIS (SO₄²⁻, NO₃⁻, NH₄⁺ and Cl⁻) using an IC, and 32 metals (Al, Na, K, Ca, Ti, V, Cr, Mn, Fe, Ni, Cu, Zn, As, Se, Rb, Sr, Zr, Cd, Sn, Sb, Ba, Pb, Cs, La, Ce, Pt, Tl, Mg, Li, Mo, Co and Pd) using an ICP-MS. More details of analytical procedures are given in the instrumentation section.

2.2.2 Online sampling

At both IITD and IITMD site, high-resolution time-of-flight aerosol mass spectrometers (HR-ToF-AMS, Aerodyne Research Inc., Billerica, MA) (Canagaratna et al., 2007; DeCarlo et al., 2006), equipped with PM_{2.5} aerodynamic lens (Peck et al., 2016) (Aerodyne Research Inc., Billerica, MA, USA) were installed inside air-conditioned laboratories. Ambient fine particulate matters were sampled through PM_{2.5} cyclone (BGI, Mesa Labs. Inc.) inlet at IITD with a flow rate of 5 lpm (l/min) using a 2.44 m long stainless-steel tubing (0.3 inch I.D and 0.4 inch O.D) and through black silicon tubing (0.19 inch I.D) at IITMD, placed 1.5 m above the rooftop. A Nafion dryer (MD-110-144P-4; Perma Pure, Halma, UK) was used to dry the ambient aerosols to maintain the output RH at 20%. At IITD, data were collected from 12th October 2019-

31st December 2019 and 2nd June 2019-21st July 2019 during winter and summer campaigns respectively. The data between 1st November and 14th November was not available, due to hardware issues in the AMS during that period. At IITMD, data were only collected during winter campaign from 25th October 2019 to 31st December 2019.

Two Xact 625i ambient metal monitors (Cooper Environmental Services, Beaverton, Oregon, USA) were installed inside temperature controlled laboratories at IITD and IITMD. Ambient aerosols were sampled through a PM_{2.5} inlet with a flow rate of 16.7 lpm. A separate sampling line of 2.44 meter (1.25 inch I.D) for the Xact which was made of aluminium was installed. A heater was set up at the end of the sampling line to ensure 45% RH set point. At IITD, sampling was carried out from 1st October 2019-31st December 2019 and 30th May 2019-25th July 2019 during the winter and summer campaign, respectively. However, data between 16th July and 24th July were not available due to hardware breakdown. At IITMD, samples were collected from 1st October 2019-31st December 2019 but data from 18th November to 26th November 2019 and 30th November to 14th December 2019 were not available due to instrumental problems.

Online measurements of inorganic ions (SO₄²⁻, NO₃⁻, NH₄⁺ and Cl⁻) from HR-ToF-AMS were compared with the WSIS using an IC. Parallely, heavy and trace metals obtained from Xact ambient metal mass monitor were compared with the metal data from the offline filter measurements using an ICP-MS. Though the sampling periods of AMS, Xact, and HVS were different for different seasons and different sites as well (Table 1), only the common periods of online and offline sampling have been discussed in this study for comparison.

Table 1. Sampling strategy and instrumentation used.

| | Interval | IITD | IITMD |
|-------------------------------|----------|---|---|
| Quartz filter Sampling | 3 days | January-May 2019 | January-May 2019 |
| | | August-September 2019 | August-September 2019 |
| | 24 hrs | June-July 2019 | June-July 2019 |
| | | October-December 2019 | October-December 2019 |
| HR-Tof-AMS | 2 mins | 2 nd June-21 st July 2019 | 25 th October-31 st December 2019 |
| | | 12 nd October-31 st December 2019 | |
| Xact | 30 mins | 30 th May-25 th July 2019 | 1 st October-31 st December 2019 |
| | | 1 st October-31 st December 2019 | |

Filters from the common periods were analysed for WSIS and heavy and trace metals using an IC and ICP-MS respectively.

2.3. Instrument details

2.3.1 WSIS measurements by IC and HR-ToF-AMS

For WSIS analysis, 9 sq.cm punch area of each collected filter was soaked in 30 ml of high purity milli-q water (resistivity-18.20 M Ω cm) for 12 hours in pre-cleaned borosilicate test tubes to ensure maximum solubility. The amount of water added, soaking time, etc. effect the solubility of the ions as well as the extent of extraction. Details can be found in our previous paper (Bhowmik et al., 2020). Soaked samples were filtered through 0.22 μ m quartz filter papers to remove any suspended contaminations after an ultrasonication for 50 mins. Cl⁻, NO₃⁻, SO₄²⁻ and, NH₄⁺ were measured for all the filter extracts by an IC (Metrohm 883 Basic IC plus for cations and 882 compact IC plus for anions). Separate columns for the analysis of cations and anions were installed in two separate modules. For anion and cation separation, an AS 5-250/4.0 chromatography column and C-6 column was used, respectively. The sample carried by 3.2 mM Na₂CO₃+1 mM NaHCO₃ solution and 2.7 mM HNO₃ solution in the anion and cation module separately passes through the charged columns to analyze each ion according to their polarity. The calibration was performed by a seven-point method with a range of standards prepared by the serial dilution from the stock solution standard of 10 ppm purchased from Metrohm. The uncertainty of the water-soluble inorganic ions measured by IC was estimated as 4% (coverage factor~2) by the approach described in Yardley et al. (2007).

HR-ToF-AMS measures size-resolved mass spectra of non-refractory particles (PM components that vaporize at 600°C and 10⁻⁵ Torr, e.g., organics, nitrate, sulphate, ammonium, and some chlorides) of submicron particulate matters. The details of this instrument can be found elsewhere (DeCarlo et al., 2006). Briefly, ambient aerosols are collected through an orifice of 100 μ m diameter and focused into a narrow particle beam by an aerodynamic lens system installed inside the instrument, which has a transmission efficiency of > 50% for PM_{2.5} (DeCarlo et al., 2006; Peck et al., 2016). The particle size is determined after analyzing the time of flight, i.e., time taken to travel along the length of the sizing chamber. The NR-PMs are then vaporized by hitting the vaporizer at 600°C and at a vacuum of 10⁻⁷ Torr. Further, the vaporized molecules are electronically ionized at 70 eV, followed by detection by a mass spectrometer as per their *m/z*. HR-ToF-AMS can be operated in W-mode or V-mode. For this study, it was operated in V-mode with a sampling time of 2 mins. Mass spectra (MS) mode, in which mass spectra of the components are measured, and particle time-of-flight (PTof) mode in which the size-resolved mass spectra are measured, are alternated in every 30s in 2 cycles. The HR-ToF-AMS was calibrated using standard protocols provided in our previous publication (Lalchandani et al., 2021; Singh et al., 2019).

To determine the mass concentration of NR-PMs, Unit mass resolution (UMR) analysis was done using the SQUIRREL data analysis toolkit (version 1.59) programmed in IGOR Pro 6.37 software (Wavemetrics, Inc., Portland, OR, USA). High resolution (HR) analysis was also done on the data set using Peak Integrated Key Analysis (PIKA version 1.19) toolkit. A recommended collection efficiency (CE) of 1 (Hu et al., 2017) was used for capture vaporizer. At the beginning and mid of each campaign at the two sites, ionization efficiency (IE) calibration was performed by injecting mono-disperse 300 nm ammonium nitrate and ammonium sulphate particles into AMS and a condensation particle counter (Jayne et al., 2000). A relative ionization efficiency (RIE) of 4.05 and 4.35 was used for IITD and IITMD site, respectively in case of NH_4 . RIE of SO_4 was taken as 2.89 and 1.67 for IITD and IITMD, respectively. For Org and Cl, by default a RIE of 1.4 and 1.3 were taken, respectively. More details can be found in (Lalchandani et al., 2022).

2.3.2 Heavy and trace metal measurements by ICP-MS and Xact 625i

For the analysis of heavy and trace metals, 15 sq. cm area of each collected filter was digested in an acid mix of 0.5 ml HF +1.5 ml HNO_3 for 4 hours within closed HDPE Teflon tubes using a Hot plate (Saville-HF resistive Model number 88888:00000). The temperature range should be $\sim 90\text{--}120^\circ\text{C}$ to ensure complete digestion of the elements. Further, 2.5 ml of HClO_4 was added to the precipitates, left over the Teflon tube wall and the tubes were kept on the hot plate at $220\text{--}240^\circ\text{C}$ for another 4 hours with the lids open for complete evaporation of the acid mix. Moreover, the residual was dissolved in 6N HNO_3 and diluted with de-ionized water (resistivity- $18.20\text{ M}\Omega\text{ cm}$) followed by filtering through $0.22\text{ }\mu\text{m}$ quartz filter papers prior analysis. Details can be found in our forthcoming paper. This method is well established and used in many studies (Minguillón et al., 2012; Querol et al., 2008).

Thirty two metals (Al, Na, K, Ca, Ti, V, Cr, Mn, Fe, Ni, Cu, Zn, As, Se, Rb, Sr, Zr, Cd, Sn, Sb, Ba, Pb, Cs, La, Ce, Pt, Tl, Mg, Li, Mo, Co and Pd) were analyzed for all filter extracts using an ICP-MS (Thermo Scientific iCAP Q ICP-MS) at IIT Kanpur Environmental Engineering laboratory. Si could not be determined in the filter samples because Si is the primary constituent of the quartz filters and hence digested during sample preparation. Samples were first introduced to a nebulizer using an injector attached to an autosampler for transformation into fine aerosol droplets followed by ionization at a very high temperature (8000K) in Ar-plasma. The elements elute as per their m/z . A known concentration (5 ppb) of Ge was used as an internal standard to monitor the instrumental drift during the analysis. The overall average drift was reported as $\pm 10\%$. The calibration was performed by ten-point method with a range of mix standards prepared by the serial dilution from the High purity multi-element (35 elements) standards (soluble in 1% HNO_3 , 100 ppm) purchased from Sigma Aldrich.

The Xact 625i Ambient Metals Monitor (Cooper Environmental Services (CES), Beaverton, OR, USA) uses X-ray fluorescence to measure the real-time elemental data in particulate matter. For this study, a PM_{2.5} inlet was used. Details of the instrument can be found in Furger et al., 2017. Briefly, aerosol samples were collected on a Teflon filter tape followed by hitting the loaded area with X-rays and the fluorescence measured by a silicon drift detector (SDD). Thirty elements: Al, Si, S, Cl, K, Ca, Ti, Cr, Mn, Fe, Co, Ni, Cu, Zn, As, Se, Br, Rb, Sr, Zr, Mo, Cd, In, Sn, Sb, Te, Ba, Pb, Bi, and Bi were measured with 30 min time resolution. The Xact 625i was calibrated during each campaign using thin film standards for the individual elements. The reproducibility was observed within $\pm 5\%$. Every midnight energy alignment checks were performed for 15 mins (00:15 to 00:30) (for Cr, Pb, Cd and Nb). An uncertainty of $\sim 10\%$ was reported by the manufacturer in an interference free situation (USEPA & Etv, 2012). This included 1.73% from flow (CEN, 2014), 5% for standard reproducibility or uncertainty during calibration (USEPA, 1999) and 2.9% from term stability as reported in Tremper et al. (2018). More details on the instrumental set up and stability check during the summer and winter campaign can be found in Rai et al. (2020) and Shukla et al. (2021).

3. Results and discussions

3.1. Online and offline measurements of WSIS and their comparison

Large temporal variability was observed in both offline and online measurements of WSIS (NO_3^- , SO_4^{2-} and, NH_4^+ and Cl^-) during the winter campaign and summer campaign at both sites. The inorganics data with 2 mins interval from HR-ToF-AMS were averaged over the sampling period of the filters, i.e., 24 hours. The time series of NO_3^- , SO_4^{2-} , NH_4^+ , and Cl^- during the summer and winter campaign at IITD and winter campaign at IITMD are shown in Fig. SM1 in the supplementary material. Higher peaks of inorganics were observed during 25th Oct-18th Nov during the winter campaign at IITD, which was the agricultural crop-residue burning period (Nagar et al., 2017). During the winter campaign, NO_3^- was the most abundant ion followed by SO_4^{2-} , NH_4^+ and Cl^- for both offline and online measurements at both the sites whereas, during the summer campaign at IITD, NO_3^- was the most abundant ion followed by NH_4^+ , SO_4^{2-} and Cl^- in online measurement (HR-ToF-AMS). Similar results were observed in our companion paper, Shukla et al. (2021). Interestingly, in the case of offline measurements during the summer campaign at IITD, NO_3^- was least abundant, and the sequence changed as $\text{SO}_4^{2-} > \text{NH}_4^+ > \text{Cl}^- > \text{NO}_3^-$. The average concentrations with their ranges are tabulated in Table SM1 in supplementary material, and the mean, maximum and minimum concentration are shown in Fig. 2 using box plots.

Comparability and correlation between offline and online measurements were evaluated in this study by applying linear regression using offline data as the independent and online data as the dependent variable. The comparability of NH_4^+ measurements was observed to be good for both summer and winter campaigns at both sites. During the winter campaign, the correlations were $R^2=0.76$, and $R^2=0.89$, and the slopes were closer to 1 (0.99 for IITD and 0.93 for IITMD) for IITD and IITMD, respectively (Fig. 3). Interestingly during the summer campaign at IITD, though the correlation improves ($R^2=0.91$), the slope decreases to 0.49. This is likely because the vapor concentration of sulfuric acid (H_2SO_4) is higher during summers. As a result of which, the adsorption of sulfuric acid on PM deposited on the filter papers happens during summers which reacts with gaseous ammonia (NH_3) to form a relatively stable particulate $(\text{NH}_4)_2\text{SO}_4$ (Zhang et al., 2000), thus increasing ammonium concentration in the offline measurements during the warmer season, especially in the presence of dust (Nicolás et al., 2009).

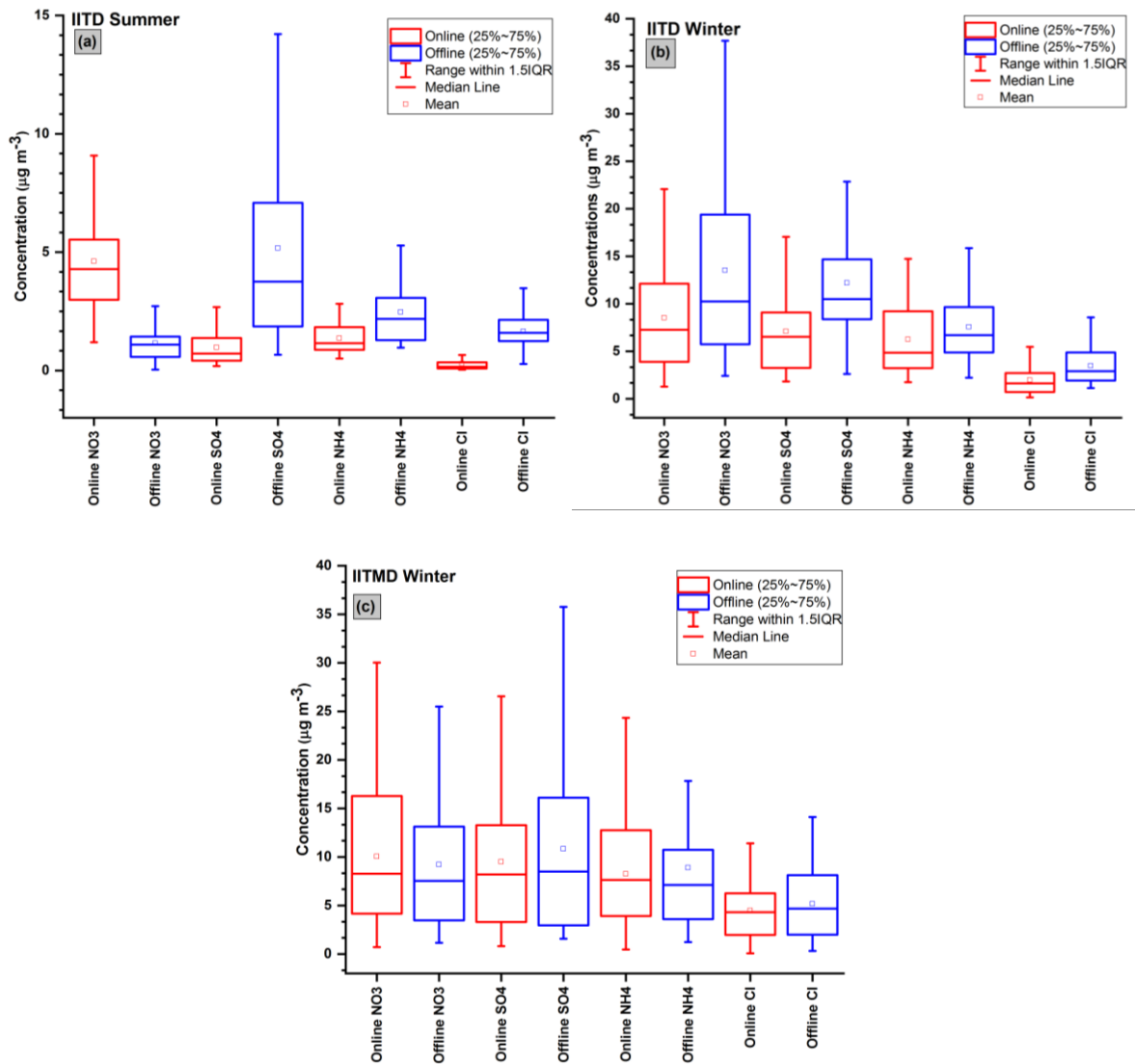
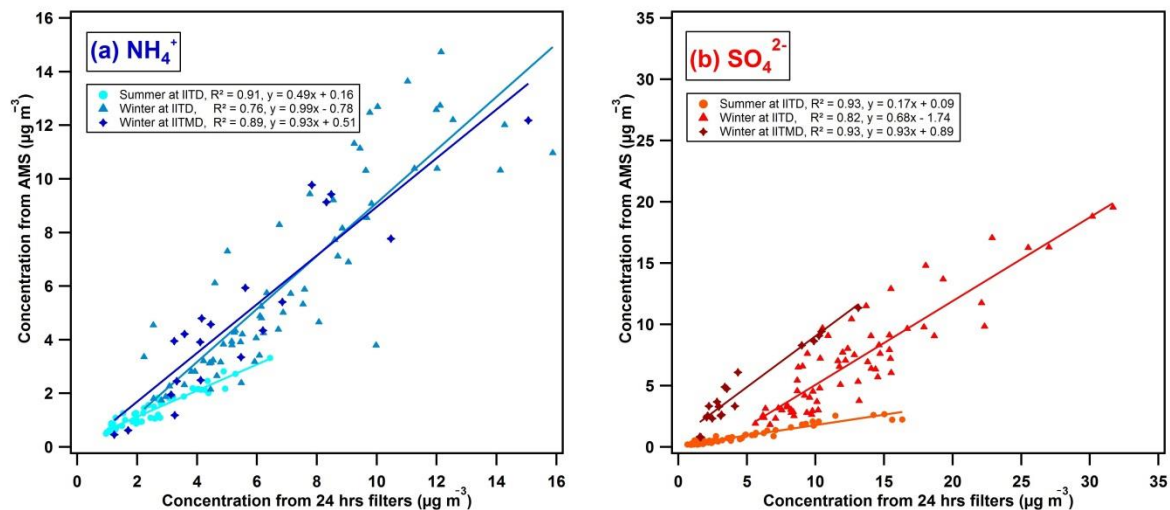


Fig.2. Box plots of online and offline measured secondary species (NO_3^- , SO_4^{2-} and, NH_4^+) and Cl^- during (a) summer campaign at IITD, (b) winter campaign at IITD, and (c) winter campaign at IITMD site.

The filter-based measurements of SO_4^{2-} were higher than those from the online measurements for IITD and IITMD during both the seasons (Fig. 2). Their comparability is characterized by a correlation coefficient of $R^2=0.93$ with a slope of 0.17 and $R^2=0.82$ with a slope of 0.68 at IITD during the summer and winter campaigns, respectively. Interestingly, offline SO_4^{2-} data correlates well with online SO_4^{2-} data having a correlation coefficient of $R^2=0.93$ with a slope close to 1 (0.93) during the winter campaign at IITMD (Fig. 3). A slope of less than 0.5 was observed in Malaguti et al., (2015) in Italy during the warm period whereas the offline measurement of SO_4^{2-} was 34% lesser than the AMS measurements in Pandolfi et al., (2014). The higher SO_4^{2-} concentrations on the un-denuded offline filter-based measurements could be due to refractory sulfate (e.g., potassium or calcium sulfate). The higher filter-sulfate could also be possibly because of the positive sampling artifact. The SO_2 is absorbed on the filter by the collected alkaline particles (Nie et al., 2010). The higher concentration could also be due to the formation of ammonium bi-sulfate or ammonium sulfate because of the reaction between gas-phase ammonia with the acidic aerosols (Nicolás et al., 2009). Also, the un-denuded filter measurements could lead to higher filter-sulfate. The interaction of gas phase ammonia with acidic aerosols can be minimized by using denuders while collecting aerosols on the filters (Nault et al., 2020). Some studies suggested that the NH_4 , SO_4 and, NO_3 measured by AMS have interferences from organics and can often be misinterpreted as fully inorganic (Chen et al., 2019; Farmer et al., 2010; Day et al., 2021). Though the interference is minimum, this could lead to possible biases between the online and offline measurement of the inorganics.



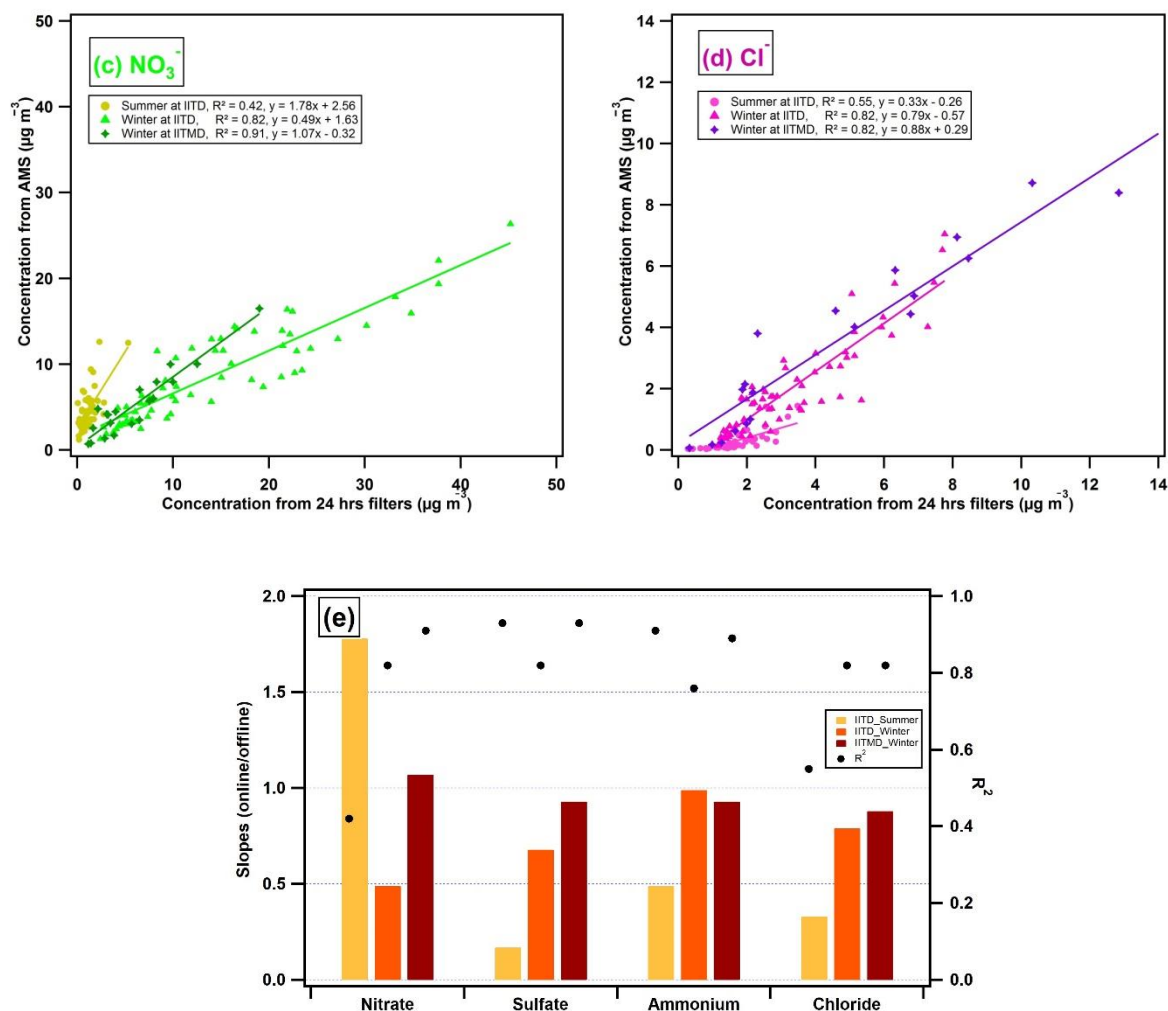


Fig.3. Scatter plots between online and offline measured (a) NH_4^+ , (b) SO_4^{2-} , (c) NO_3^- , (d) Cl^- concentrations and (e) comparison of slopes (online/offline) and R^2 of the measured inorganic ions in $\text{PM}_{2.5}$ during summer and winter campaign at IITD and during winter campaign at IIITMD.

The online and offline NO_3^- measurements posed a good correlation during winter ($R^2 = 0.91$ and slope of 1.07 at IITMD, $R^2 = 0.82$ and slope of 0.49 at IITD) whereas the correlation worsens during summer at IITD ($R^2 = 0.42$ and slope of 1.78) (Fig. 3). The slopes and correlation coefficient for the WSIS are listed in Table 2. The NO_3^- concentrations measured by the HR-ToF-AMS were higher than the offline data during summer at IITD and during winter at IITMD whereas, filter-based measurements of NO_3^- were higher during winter at IITD (Fig. 2). The higher offline NO_3^- concentrations during winter at IITD can be possibly because of the positive artifact due to the absorption of gas-phase nitric acid (HNO_3) on the filter (Chow, 1995). Many studies (Chow et al., 2008; Kuokka et al., 2007; Malaguti et al., 2015) reported higher concentrations of NO_3^- from high time resolution measurements than filter-based measurements

due to the evaporation of ammonium nitrate collected on filters over the duration of sample collection (Pakkanen & Hillamo, 2002; Schaap et al., 2004; Kuokka et al., 2007). Pandolfi et al. (2014) observed NO_3^- HR-AMS/Filter ratios of ~ 1.7 at Barcelona and Montseny in Europe. This evaporation loss increases with the decrease of humidity and the increase of temperature (Chow et al., 2008; Takahama et al., 2004). Also, complete evaporation may occur beyond 25°C (Schaap et al., 2004). Chow et al. (2008) observed the evaporation loss from quartz filter to be more than 80% during the warm season in central California. The high temperature (35°C - 48°C) during the long sampling hours (24 hours) may be a possible reason for the poor correlation between online and offline NO_3^- measurements during the summer campaign at IITD. Schaap et al. (2004) reported that the NO_3^- volatilization during a 24-h sampling period not only depends on the sampling instruments and ambient conditions, but also on sampling strategy. If the sampling strategy is evening to evening (24 hours), the samples will lose the NO_3^- sampled during night with the increasing temperature during the day. However, during morning-to-morning sampling strategy, the filters will collect the NO_3^- quantitatively at night, and the higher temperature in the afternoon of the previous day may promote the loss of NO_3^- from the filter (Malaguti et al., 2015). In this study, the sampling time was from 6:30 am to the next day 6.30 am. Therefore, the filter-based inorganic measurements suffered from a negative sampling artifact due to the evaporation of nitrate collected during the forenoon in a temperature of 20°C - 25°C during the winter campaign and $\sim 38^\circ\text{C}$ - 45°C during the summer campaign.

Table 2. Regression coefficients and slopes for the comparison of WSIS measured by HR-ToF-AMS and IC.

| Sites | NO_3^- | | SO_4^{2-} | | NH_4^+ | | Cl^- | |
|---------------------|-----------------|-------|--------------------|-------|-----------------|-------|---------------|-------|
| | R^2 | Slope | R^2 | Slope | R^2 | Slope | R^2 | Slope |
| IITD Summer | 0.42 | 1.78 | 0.93 | 0.17 | 0.91 | 0.49 | 0.55 | 0.33 |
| IITD Winter | 0.82 | 0.49 | 0.82 | 0.68 | 0.76 | 0.99 | 0.82 | 0.79 |
| IITMD Winter | 0.91 | 1.07 | 0.93 | 0.93 | 0.89 | 0.93 | 0.82 | 0.88 |

We observed higher Cl^- concentration in filter-based measurement than online measurement using HR-ToF-AMS during both campaigns at IITD and winter at IITMD. A good correlation of $\text{R}^2 = 0.82$ with a slope of 0.79 and $\text{R}^2 = 0.82$ with a slope of 0.88 was observed during the winter campaign at IITD and IITMD, respectively (Fig. 3). Interestingly, during the summer campaign at IITD the comparability was moderate with a correlation coefficient of $\text{R}^2 = 0.55$ and a slope of 0.33. A correlation coefficient of $\text{R}^2 = 0.83$ between $\text{Dp} < 10 \mu\text{m}$ measured with the MARGA and analyzed from Teflon filters was reported in Makkonen et al., (2012) during Feb-May. Lower temperature and higher RH during winter retains Cl^- in particulate phase for long enough to be detected which is not the case in summer. Further, Cl^- is

predominantly found in the coarse fraction. Also, while AMS only measures the NR-Cl⁻ (Manchanda et al., 2021), e.g. NH₄Cl, which can vaporize at 600°C but cannot measure Cl⁻ from refractory-KCl, IC measures chloride from all the water-soluble chloride salts, including NH₄Cl and KCl. This probably justifies the lower concentration of Cl⁻ in online measurement from AMS than filter-based measurements. We also compared Cl⁻ measurements from Xact 625i with the measurements from IC. Interestingly, IC measurements of Cl⁻ were found to be higher than Xact 625i measurements during summer at IITD and winter at IITMD. The Cl measurements from Xact 625i were ~1.9 times higher than the measurements from IC during winter at IITD (see fig. SM2 in supplementary material). The correlations were found to be good during winter ($R^2 = 0.83$ and 0.76 at IITD and IITMD respectively) and worsen during summer ($R^2 = 0.27$ at IITD), similar to what we observed for AMS-Cl⁻ and IC-Cl⁻. It could be due to the differences in water-soluble fraction of chloride in the samples, as ionic concentration (IC) represents water-soluble fraction whereas elemental concentration (Xact 625i) represents total concentration. Also, a lot particulate bound chloride in the atmosphere is in the form of ammonium chloride (Manchanda et al., 2021). Part of the ammonium chloride collected during the day long offline sampling would have vaporized, giving lower concentration from IC measurements. Further investigation is needed to draw a firm conclusion.

3.2 Online and offline measurements of heavy and trace metals and their comparison

For the inter-comparison of heavy and trace metal concentrations from Xact 625i and ICP-MS, the half-hourly Xact 625i data were averaged to 24 hours filter sampling interval. A total of 32 elements were analyzed on each filter using ICP-MS while, 27 elements were measured in Xact 625i at IITD during summer and winter campaign, and 30 elements were measured in Xact 625i at IITMD during the winter campaign. The spatial and temporal variations of the crustal and trace elements are shown in Fig. SM3. Al and Ca concentrations were the most abundant in ICP-MS and Xact measurements respectively during the summer season (Fig. 4a, 5a & 5b) because of the increase in the crustal activities whereas K concentrations were significantly high for both the measurements during winter (Fig. 4d, 4g, 5c, 5d, 5e and 5f) due to mass-scale agricultural crop-residue burning in the adjoining states of Punjab and Haryana. Elements emitted from anthropogenic activities, e.g., coal-fired power plants (As, Se, Hg, Pb), traffic emissions (Cr, Pb, Mn), wear debris emission (Cu, Cd, Fe, Ga, Mn, Mo), etc. are found to be in higher concentration during winter campaign than summer campaign for both the measurements. Similar results were observed in our companion paper Shukla et al. (2021). The average values of metals along with their ranges are tabulated in Table SM2 and the statistics involved mean, upper, and lower values of some major elements are shown in Fig. 4. Box plots for rest of the metals can be found in Fig. SM4.

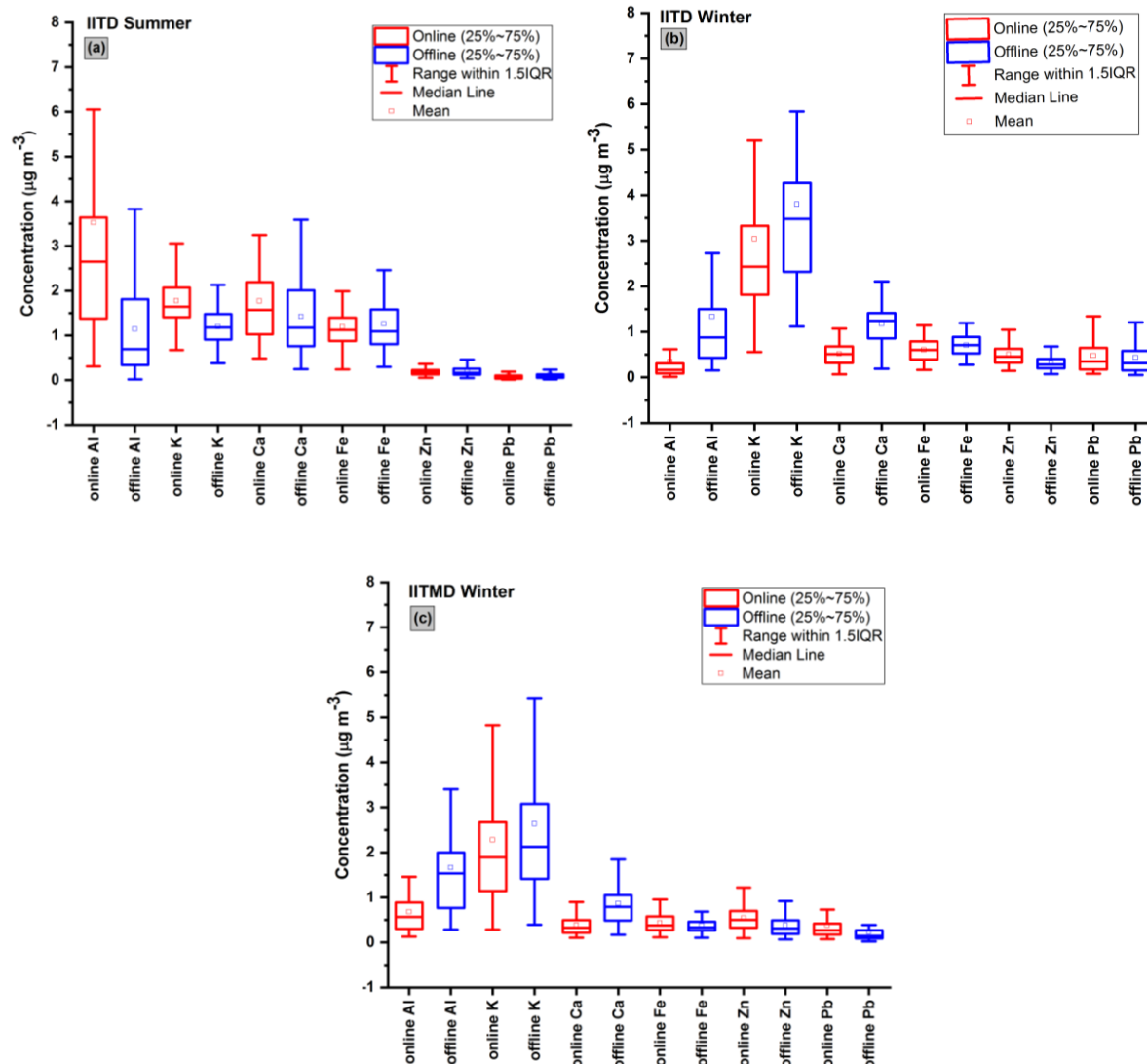


Fig.4. Box plots of some major elements measured offline and online during (a) summer campaign at IITD, (b) winter campaign at IITD, and (c) winter campaign at IITMD site. The box plots for rest of the heavy and trace elements are shown in fig. SM4 of the supplementary material.

The trends of the elemental concentration in decreasing order for both ICP-MS and Xact measurements during summer and winter at IITD and winter at IITMD are shown in Fig. SM5. The trace metals such as Cd, Mn, Mo, Ba, Pd etc. contribute a small portion in $\text{PM}_{2.5}$ in terms of their mass concentration but have a significant effect on human health. Fractions of elements in total element concentration for both the measurements during summer and winter campaign at IITD and during winter campaign at IITMD were shown in Fig. 5.

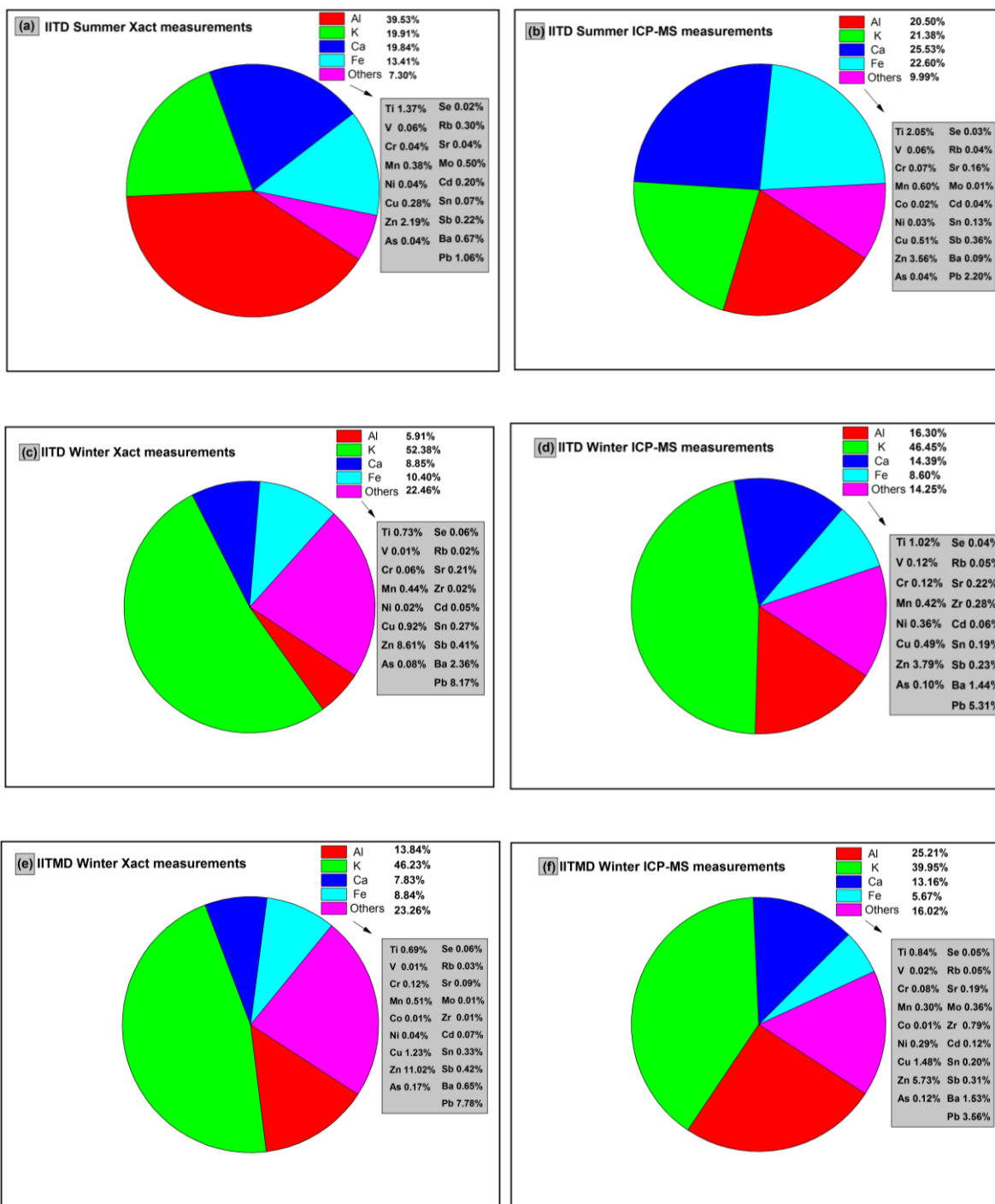
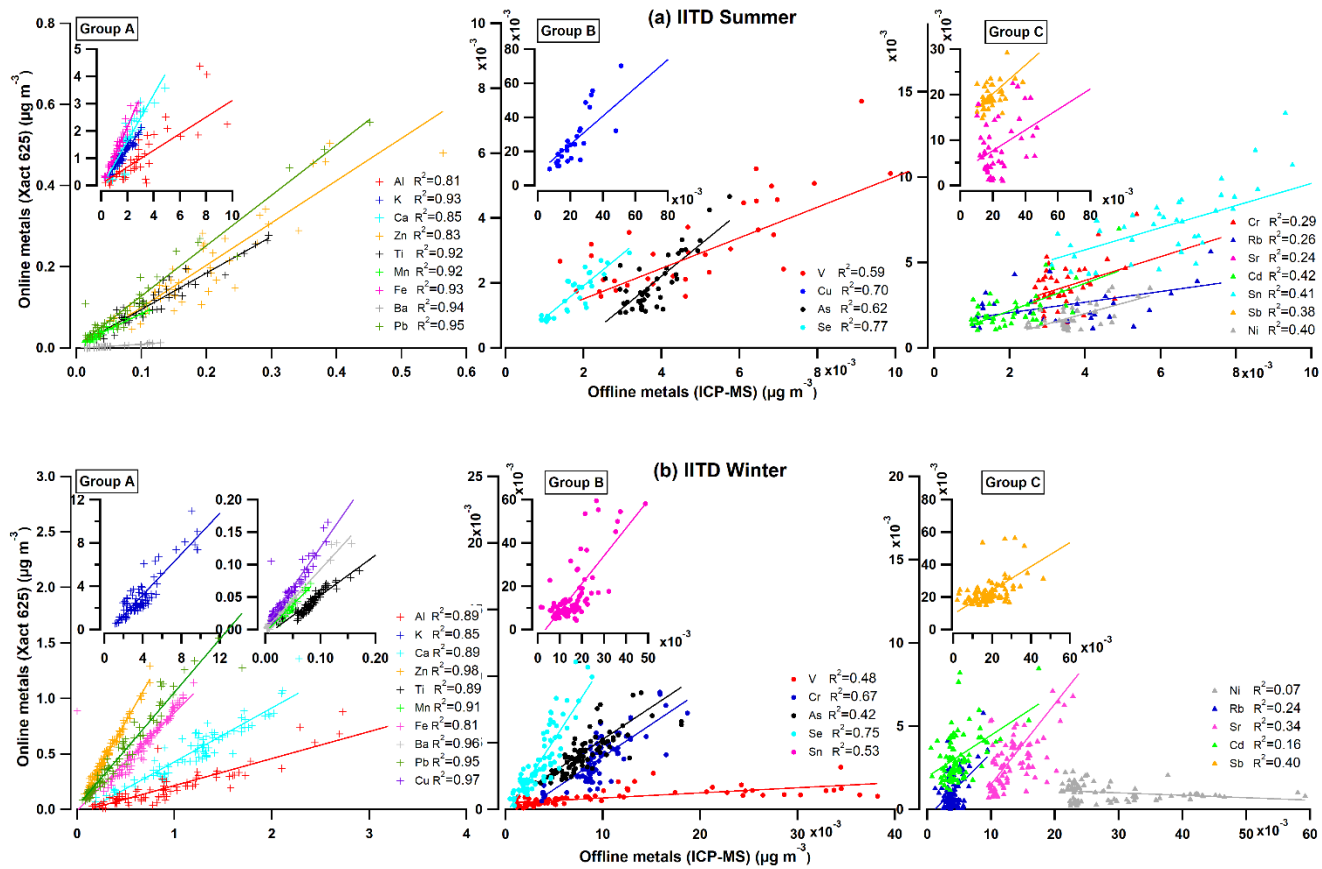


Fig.5. Fractions (%) of elements in total element concentration in $PM_{2.5}$ presented in pie format for online (a,c,e) and offline (b,d,f) measurements during winter and summer at IITD and during winter at IITMD.

MDLs for ICP-MS measurements were calculated according to Escrig Vidal et al., (2009), and MDLs for Xact 625i were obtained from the manufacturer. MDLs for the Xact 625i and ICP-MS are listed in Table

SM2 in the supplementary material. Though the half-hourly Xact data were averaged to 24 hours to the corresponding interval of the filter sampling, for comparability check, MDLs of Xact 625i measurements were taken for 30 mins sampling time while MDLs of filter-based elemental measurements were calculated for 24 hours. Elements having data below $3 \times \text{MDL}$ were discarded from further examination and unreliable as values below $3 \times \text{MDL}$ would lead to higher uncertainty (Furger et al., 2017). The elements K, Ca, Ti, Mn, Fe, Ba, and Pb have >80% of their values above both offline and online MDLs, and thus the data quality is reliable. Further, Ni, Mo, Zr have higher blank concentrations, and thus the data is not reliable for ICP-MS measurements. The comparability of the elements measured online using Xact 625i with those analysed using an ICP-MS, was checked for the common elements in these two measurements (21 elements for IITD and 23 elements for IITMD) and is shown in Fig. 6.



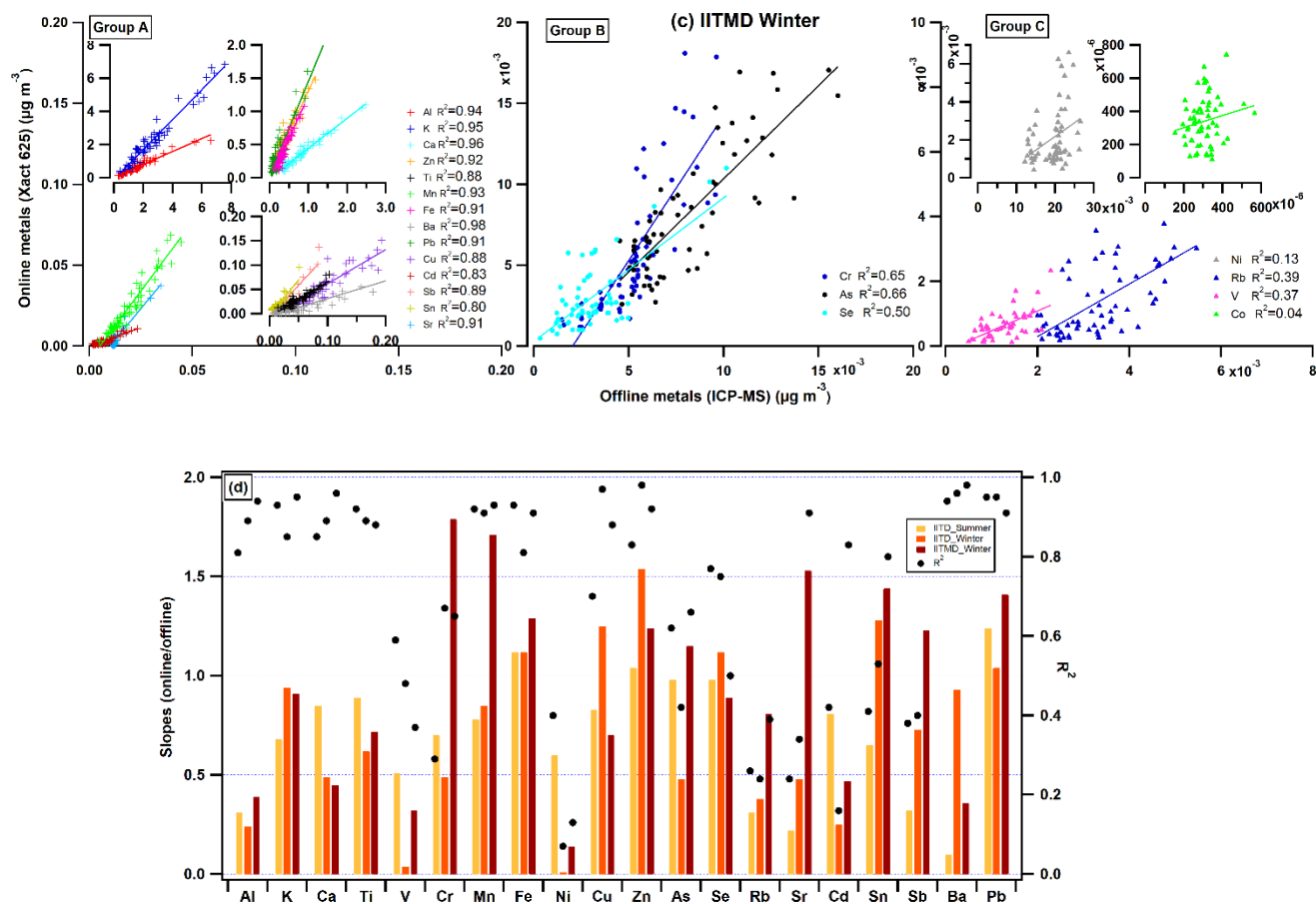


Fig. 6. Scatter plots and regression lines of Xact 625i vs. ICP-MS data for groups A, B, and C during (a) summer at IITD, (b) winter at IITD, (c) winter at IITMD, and (d) comparison of slopes (online/offline) & R^2 of the measured heavy and trace metals in $PM_{2.5}$ during the summer and winter campaign at IITD and winter campaign at IITMD.

Based on their comparability characteristics, elements were grouped under 3 categories. Group A showed excellent linearity between the two methods with a correlation coefficient of $R^2 > 0.8$. Overall, group A consists of Al, K, Ca, Ti, Mn, Fe, Cu, Zn, Ba, and Pb during winter at IITD whereas, Cu showed in another group during summer at IITD. Though Sr, Cd, Sn, Sb had average values below MDLs and posed a lower correlation coefficient at IITD, interestingly, Sr, Cd, Sn, and Sb joined group A during winter at IITMD. To distinguish the potential difference in accuracy between the two methods, intercepts were not forced to be zero. The slopes are important, which indicate biases between the two measurements. The slopes of Zn, Fe, and Pb were closer to unity during summer at IITD (Fig. 6). K, Fe, Cu, Zn, Ba, and Pb achieved a slope of 0.94-1.25 during winter at IITD whereas, Mn, Fe, Zn, Pb, Sr, Sn, and Sb pose a slope slightly higher than unity during winter at IITMD (Fig. 6). A slight difference in cut-off value for the

particle size can reduce the slopes from unity and produce ~10% difference in collected mass (Panteliadis et al., 2012). The slopes and the correlation coefficients are listed in Table 3.

In a comparison study conducted by USEPA & Etv. (2012) between Xact 625i and ICP-MS measurements, Ca, Cu, Mn, Pb, Se, and Zn were highly correlated except Cu. Cu was close to the MDL values of ICP-MS and Xact 625i. A good agreement was observed between Xact 625i and offline measurements using ED-XRF in South Korea by Park et al., (2014). The comparability between Xact measurements and ICP-MS measurements was checked for the elements As, Ba, Ca, Cr, Cu, Fe, K, Mn, Ni, Pb, Se, Sr, Ti, V, and Zn in Tremper et al. (2018). They observed an average R^2 of 0.93 and a slope of 1.07 for these elements. In the study by Furger et al., (2017) during a warmer season in Switzerland, an excellent correlation ($R^2 > 0.95$) was found for Xact and ICP-OES/MS measurements of S, K, Ca, Ti, Mn, Fe, Cu, Zn, Ba, and Pb. However, they found that the elemental measurements by Xact 625i were 28% higher than ICP-OES/MS measurements for these 10 elements. In our study, Xact measurements of Fe, Cu, Zn, and Pb yielded an average of 24% higher mass concentrations than ICP-MS measurements for Group A elements during winter at IITD. Xact measurements were systematically 10% (average) higher than ICP for Zn, Fe, and Pb during summer at IITD, whereas; we obtained an average of 41% higher Xact measurements than ICP for Mn, Fe, Zn, Pb, Sr, Sn, and Sb during winter at IITMD in Group A elements.

Group B was characterized by moderate linearity having $R^2 \sim 0.4-0.8$ and consisted of the elements V, Cu, As, and Se during summer at IITD; V, Cr, As, Se, Sn during winter at IITD and Cr, As and Se during winter at IITMD. These elements in Group B had their values very close to or below MDLs of at least one of the analysis methods. During winter at both sites, Cr and As from ICP-MS have ~50-65% of their values below MDLs, whereas ~68-72% of their values were above the MDLs of Xact 625i. Though some of the elements in this group in different seasons have slopes near or greater than unity (see Table 3) like Group A, their comparison is not statistically feasible.

Table 3. Regression coefficients and slopes for the comparison of Xact 625i and ICP-MS measurements.

| Sites | Group A | Slope | R^2 | Group B | Slope | R^2 | Group C | Slope | R^2 |
|-------------|---------|-------|-------|---------|-------|-------|---------|-------|-------|
| IITD Summer | Al | 0.31 | 0.81 | V | 0.51 | 0.59 | Cr | 0.7 | 0.29 |
| | K | 0.68 | 0.93 | Cu | 0.83 | 0.70 | Co | - | - |
| | Ca | 0.85 | 0.85 | As | 0.98 | 0.62 | Rb | 0.31 | 0.26 |
| | Zn | 1.04 | 0.83 | Se | 0.98 | 0.77 | Sr | 0.22 | 0.24 |
| | Ba | 0.1 | 0.94 | | | | Mo | - | - |

| | | | | | | | | | |
|---------------------|----|------|------|----|------|------|----|------|------|
| | Ti | 0.89 | 0.92 | | | | Cd | 0.81 | 0.42 |
| | Mn | 0.78 | 0.92 | | | | Sn | 0.65 | 0.41 |
| | Fe | 1.12 | 0.93 | | | | Sb | 0.32 | 0.38 |
| | Pb | 1.24 | 0.95 | | | | Ni | 0.6 | 0.4 |
| IITD Winter | Al | 0.24 | 0.89 | V | 0.04 | 0.48 | Ni | 0.01 | 0.07 |
| | K | 0.94 | 0.85 | Cr | 0.49 | 0.67 | Rb | 0.38 | 0.24 |
| | Ca | 0.49 | 0.89 | As | 0.48 | 0.42 | Sr | 0.48 | 0.34 |
| | Ti | 0.62 | 0.89 | Se | 1.12 | 0.75 | Zr | - | - |
| | Mn | 0.85 | 0.91 | Sn | 1.28 | 0.53 | Cd | 0.25 | 0.16 |
| | Fe | 1.12 | 0.81 | | | | Sb | 0.73 | 0.40 |
| | Cu | 1.25 | 0.97 | | | | | | |
| | Zn | 1.54 | 0.98 | | | | | | |
| | Ba | 0.93 | 0.96 | | | | | | |
| | Pb | 1.04 | 0.95 | | | | | | |
| IITMD Winter | Al | 0.39 | 0.94 | Cr | 1.79 | 0.65 | Ni | 0.14 | 0.13 |
| | K | 0.91 | 0.95 | As | 1.15 | 0.66 | Rb | 0.81 | 0.39 |
| | Ca | 0.45 | 0.96 | Se | 0.89 | 0.5 | Mo | - | - |
| | Ti | 0.72 | 0.88 | | | | Zr | - | - |
| | Mn | 1.71 | 0.93 | | | | V | 0.32 | 0.37 |
| | Fe | 1.29 | 0.91 | | | | Co | 0.36 | 0.04 |
| | Cu | 0.70 | 0.88 | | | | | | |
| | Zn | 1.24 | 0.92 | | | | | | |
| | Ba | 0.36 | 0.98 | | | | | | |
| | Pb | 1.41 | 0.91 | | | | | | |
| | Sr | 1.53 | 0.91 | | | | | | |
| | Cd | 0.47 | 0.83 | | | | | | |
| | Sn | 1.44 | 0.8 | | | | | | |
| | Sb | 1.23 | 0.89 | | | | | | |

469 The Group C elements, e.g., Ni, Rb, Sr, Zr, Cd, and Sb during summer at IITD; Cr, Co, Rb, Sr, Mo, Cd,
470 Sn, Sb, and Ni during winter at IITD and, Ni, Rb, Mo, Zr, V, and Co during winter at IITMD are
471 characterized by their bad correlation ($R^2 < 0.4$). Interestingly, measurements of some element e.g. Mo
472 during summer and winter at IITD and IITMD respectively, Co during summer at IITD, and Zr during

winter at both sites from both the methods did not correlate at all. For most of the elements in this group, 70-85% of measurements were below both method's MDLs and rest of the data were below $3 \times$ MDLs. The high and variable blank concentrations of these elements increased the MDL values in ICP-MS measurement. The particle size dependent self-absorption effect and line interference between different elements in Xact measurement could also increase the MDL values (Furger et al., 2017). This is probably the reason for the values lower than MDLs for the elements in this group.

Overall, we observed 10-40% higher Xact measurements than ICP for some of the elements in Group A during different seasons. The difference in the Xact and High-volume sampler inlet location and their distance from the road can cause such difference in measurements (Furger et al., 2017). In the case of dust resuspension from vehicular traffic, the number concentration of finer particulate matter tends to decrease sharply within an increment of just 50m from the roadway (Hagler et al., 2009). In this study, we tried to co-locate the two sample inlets, but it could not be avoided. Also, IITD and IITMD are both very close (<200 m) to a roadway with moderate to heavy-duty traffic. The differences in online and offline measurements may indicate a gradient in some elements due to very close proximity to heavy-duty traffic. Also, the different temperatures of the sample inlets may give rise to a difference in measured concentrations from both methods (Tremper et al., 2018). In this study, the blank corrected ICP-MS measurements may result in overestimation or underestimation due to variable and high blank concentration. The difference can also occur due to the digestion recovery rate for the digestion protocol used for the filter analysis. Moreover, if the ambient elemental concentration is much lower than the standards used for calibration of Xact, such differences may occur (Indresand et al., 2013).

4. Conclusion

Atmospheric WSIS (NO_3^- , SO_4^{2-} , NH_4^+ , Cl^-) and heavy and trace elements in $\text{PM}_{2.5}$ were measured using offline methods (IC for WSIS and ICP-MS for elements) and online methods (HR-ToF-AMS for inorganics and Xact 625i for elements). These measurements were compared to assess the measurement quality and sampling artifacts of these measurement techniques in the heavily polluted Delhi-NCR for two different metrological conditions (winter and summer season). Field campaigns were conducted at two NCR sites, namely, IITD during June-July 2019 and Oct-Dec 2019 and at IITMD during Oct-Dec 2019. The key findings of this study are summarized below.

- NH_4^+ concentrations from the IC and HR-ToF-AMS, compared well during winter with a slope of 0.99 at IITD and 0.93 at IITMD. Interestingly, NH_4^+ concentrations were higher in offline

measurements during summer at IITD. The decrease in slope was probably due to the formation of particulate $(\text{NH}_4)_2\text{SO}_4$.

- Offline SO_4^{2-} measurements were higher (with a slope of 0.17 during summer at IITD and 0.8 and 0.93 during winter at IITD and IITMD, respectively) during both seasons at both the sites due to the positive sampling artifact. The absorption of SO_2 and the oxidation or condensation process may result in additional sulphate.
- Lower NO_3^- concentrations (with a slope of 1.78 during summer at IITD and 1.07 during winter at IITMD) were observed in the offline measurement during summer at IITD and during winter at IITMD because of the evaporation of NH_4NO_3 from the filter substrates. The evaporative loss of nitrate from the filters was minimal in winter at IITMD. It aggravated during summer at IITD due to the evaporation of ammonium nitrate in such a high temperature (35°C - 48°C) range. The higher NO_3^- concentrations (slope~0.49) in the filters than HR-ToF-AMS measurements during winter at IITD can be due to the absorption of gas-phase HNO_3 on the filter.
- Offline Cl^- was consistently higher (with a slope of 0.33 during summer at IITD and 0.79 and 0.88 during winter at IITD and IITMD, respectively) than HR-ToF-AMS measurements during both seasons at both sites mainly because HR-ToF-AMS only measures the NR- Cl^- whereas, the offline Cl^- measurements includes chloride from all the water-soluble chloride salts. The comparability degrades during summer due to the volatile nature of Cl^- in higher temperatures and lower RH.
- The elements were grouped into three categories (Group A, B and C) according to their comparability characteristics. The elemental data from Xact 625i were highly correlated ($R^2>0.8$) with ICP-MS measurements of the 24 hr filters for Group A elements (Al, K, Ca, Ti, Zn, Mn, Fe, Ba, and Pb). The Cu also showed up in this group during winter at IITD. About 80% of the data for these elements were above MDLs for both the methods. Though Sn, Sb, and Cd had values below MDLs of one or both the methods, interestingly, they were highly correlated ($R^2>0.8$) and, slopes are very close to unity for Sn and Sb during winter at IITMD. The correlation coefficients > 0.8 for the elements in Group A indicated the high precision of the online and offline measurements. Hence, these elements from any of these methods can be reliably used for modelling studies.
- The elements under Group B had their values closer to or below at least one of the method's MDLs. Cr and As had ~50-65% of their values below ICP-MS MDLs from ICP-MS, whereas ~68-72% of their values were above Xact 625i MDLs during winter at both sites.

- Elements like Ni, Mo, and Zr measured from ICP-MS were not reliable due to their higher and variable blank concentrations. No conclusion on their measurement accuracy by the two methods can be drawn.
- In summary, the daily averaged half-hourly Xact 625i measurements were 10-40% higher than 24 hr filter measurements by ICP-MS depending upon the seasons, sites and elements in Group A. Distance between two inlets for the two methods, distance of the inlets from the roadway, line interference between two elements in Xact measurements, particle size, sampling strategy, filter type, higher and variable concentrations in blank filters and digestion protocol for ICP measurements can cause the difference in measurements between the two methods.

The above findings highlight the measurement methods' accuracy and implement the particular type of measurements as needed. Denuders could be effective in avoiding the overestimation problems of ammonium and sulphate in filter measurements and improve the comparison. Also, teflon filters instead of quartz filters in the un-denuded sampler are reported to give better comparison for sulphate. The MDLs in the Xact 625 measurements are higher than the MDLs for the offline method. Depending on the objective of the campaign, Xact 625 can be deployed for a longer time interval to analyse the elements that are below their MDLs. The high resolution real-time monitoring of non-refractory organics, inorganics by HR-ToF-AMS and elements by Xact comes at the cost of high sensitivity in MDLs, calibrations and cost. Whereas, cost effectiveness of conventional samplers makes it practical to deploy in larger numbers at multi-sites simultaneously. Overall, high resolution real time sampling provides a rich dataset for high and small pollution episodes. Future work should involve using different filter substrates and different digestion protocols to re-evaluate the difference between these online and offline methods. Although this study compares the PM species, a comparison of full source apportionment analysis between online and offline methods should be done for more qualitative and quantitative insights.

Author contribution

HSB performed the offline analysis, data processing and wrote the manuscript. JD collected the AMS data at IITD. AS and VL carried out the Xact and AMS data collection and processing respectively. NR, MK, VS and SNT were involved with the supervision and conceptualization. All co-authors contributed to the paper discussion and revision.

Declaration of interests

The authors declare that they have no conflict of interest.

Acknowledgements

The authors are thankful to Naba Hazarika and Mohd Faisal for collecting the Xact data at IITMD and Pawan Vats for the sampling and collection of the filters at IITD. The authors are also thankful to Amit Vishwakarma, Vaibhav Shrivastava and Harishankar for helping in offline analysis. This work is financially supported by the Department of Biotechnology, Government of India (Grant No. BT/IN/UK/APHH/41/KB/2016-17 dated 19th July 2017) and Central Pollution Control Board (CPCB), Government of India to conduct this research under grant no. AQM/Source apportionment_EPC Project/2017 dated 12th February 2019.

Reference

- Bhowmik, H. S., Naresh, S., Bhattu, D., Rastogi, N., Prévôt, A. S. H., & Tripathi, S. N. (2020). Temporal and spatial variability of carbonaceous species (EC; OC; WSOC and SOA) in PM_{2.5} aerosol over five sites of Indo-Gangetic Plain. *Atmospheric Pollution Research*, 12(June 2020), 375–390. <https://doi.org/10.1016/j.apr.2020.09.019>
- Chen, Y., Xu, L., Humphry, T., Hettiyadura, A. P. S., Ovadnevaite, J., Huang, S., Poulain, L., Schroder, J. C., Campuzano-Jost, P., Jimenez, J. L., Herrmann, H., O'Dowd, C., Stone, E. A., & Ng, N. L. (2019). Response of the Aerodyne Aerosol Mass Spectrometer to Inorganic Sulfates and Organosulfur Compounds: Applications in Field and Laboratory Measurements. *Environmental Science and Technology*, 53(9), 5176–5186. <https://doi.org/10.1021/acs.est.9b00884>
- Chow, J. C. (1995). Measurement methods to determine compliance with ambient air quality standards for suspended particles. *Journal of the Air and Waste Management Association*, 45(5), 320–382. <https://doi.org/10.1080/10473289.1995.10467369>
- Chow, J. C., Watson, J. G., Lowenthal, D. H., Park, K., Doraiswamy, P., Bowers, K., & Bode, R. (2008). Continuous and filter-based measurements of PM_{2.5} nitrate and sulfate at the Fresno Supersite. *Environmental Monitoring and Assessment*, 144(1–3), 179–189. <https://doi.org/10.1007/s10661-007-9987-5>
- Day, D., Campuzano-Jost, P., Nault, B., Palm, B., Hu, W., Guo, H., Wooldridge, P., Cohen, R., Docherty, K., Huffman, J. A., de Sá, S., Martin, S., & Jimenez, J. (2021). A Systematic Re-evaluation of Methods for Quantification of Bulk Particle-phase Organic Nitrates Using Real-time Aerosol Mass Spectrometry. *Atmospheric Measurement Techniques Discussions*, 2(3), 1–35. <https://doi.org/10.5194/amt-2021-263>
- DeCarlo, P. F., Kimmel, J. R., Trimborn, A., Northway, M. J., Jayne, J. T., Aiken, A. C., Gonin, M., Fuhrer, K., Horvath, T., Docherty, K. S., Worsnop, D. R., & Jimenez, J. L. (2006). Field-deployable, high-resolution, time-of-flight aerosol mass spectrometer. *Analytical Chemistry*, 78(24), 8281–8289.

596 <https://doi.org/10.1021/ac061249n>

597 Escrig Vidal, A., Monfort, E., Celades, I., Querol, X., Amato, F., Minguillón, M. C., & Hopke, P. K. (2009).
 598 Application of optimally scaled target factor analysis for assessing source contribution of ambient PM₁₀.
 599 *Journal of the Air and Waste Management Association*, 59(11), 1296–1307. [https://doi.org/10.3155/1047-](https://doi.org/10.3155/1047-3289.59.11.1296)
 600 3289.59.11.1296

601 Farmer, D. K., Matsunaga, A., Docherty, K. S., Surratt, J. D., Seinfeld, J. H., Ziemann, P. J., & Jimenez, J. L.
 602 (2010). Response of an aerosol mass spectrometer to organonitrates and organosulfates and implications for
 603 atmospheric chemistry. *Proceedings of the National Academy of Sciences of the United States of America*,
 604 107(15), 6670–6675. <https://doi.org/10.1073/pnas.0912340107>

605 Furger, M., Minguillón, M. C., Yadav, V., Slowik, J. G., Hüglin, C., Fröhlich, R., Petterson, K., Baltensperger, U.,
 606 & Prévôt, A. S. H. (2017). Elemental composition of ambient aerosols measured with high temporal resolution
 607 using an online XRF spectrometer. *Atmospheric Measurement Techniques*, 10(6), 2061–2076.
 608 <https://doi.org/10.5194/amt-10-2061-2017>

609 Gani, S., Bhandari, S., Seraj, S., Wang, D. S., Patel, K., Soni, P., Arub, Z., Habib, G., Hildebrandt Ruiz, L., & Apte,
 610 J. S. (2019). Submicron aerosol composition in the world's most polluted megacity: The Delhi Aerosol
 611 Supersite study. *Atmospheric Chemistry and Physics*, 19(10), 6843–6859. [https://doi.org/10.5194/acp-19-](https://doi.org/10.5194/acp-19-6843-2019)
 612 6843-2019

613 Hagler, G. S. W., Baldauf, R. W., Thoma, E. D., Long, T. R., Snow, R. F., Kinsey, J. S., Oudejans, L., & Gullett, B.
 614 K. (2009). Ultrafine particles near a major roadway in Raleigh, North Carolina: Downwind attenuation and
 615 correlation with traffic-related pollutants. *Atmospheric Environment*, 43(6), 1229–1234.
 616 <https://doi.org/10.1016/j.atmosenv.2008.11.024>

617 Hong, C., Zhang, Q., Zhang, Y., Davis, S. J., Tong, D., Zheng, Y., Liu, Z., Guan, D., He, K., & Schellnhuber, H. J.
 618 (2019). Impacts of climate change on future air quality and human health in China. *Proceedings of the*
 619 *National Academy of Sciences of the United States of America*, 116(35), 17193–17200.
 620 <https://doi.org/10.1073/pnas.1812881116>

621 Hu, W., Campuzano-Jost, P., Day, D. A., Croteau, P., Canagaratna, M. R., Jayne, J. T., Worsnop, D. R., & Jimenez,
 622 J. L. (2017). Evaluation of the new capture vaporizer for aerosol mass spectrometers (AMS) through field
 623 studies of inorganic species. *Aerosol Science and Technology*, 51(6), 735–754.
 624 <https://doi.org/10.1080/02786826.2017.1296104>

625 Indresand, H., White, W. H., Trzepla, K., & Dillner, A. M. (2013). Preparation of sulfur reference materials that
 626 reproduce atmospheric particulate matter sample characteristics for XRF calibration. *X-Ray Spectrometry*,
 627 42(5), 359–367. <https://doi.org/10.1002/xrs.2456>

628 Jayne, J. T., Leard, D. C., Zhang, X., Davidovits, P., Smith, K. A., Kolb, C. E., & Worsnop, D. R. (2000).
629 Development of an aerosol mass spectrometer for size and composition analysis of submicron particles. In
630 *Aerosol Science and Technology* (Vol. 33, Issues 1–2, pp. 49–70). <https://doi.org/10.1080/027868200410840>

631 Jimenez, J. L., Jayne, J. T., Shi, Q., Kolb, C. E., Worsnop, D. R., Yourshaw, I., Seinfeld, J. H., Flagan, R. C., Zhang,
632 X., Smith, K. A., Morris, J. W., & Davidovits, P. (2003). Ambient aerosol sampling using the Aerodyne
633 aerosol mass spectrometer. *Journal of Geophysical Research: Atmospheres*, 108(7).
634 <https://doi.org/10.1029/2001jd001213>

635 Lalchandani, V., Srivastava, D., Dave, J., Mishra, S., Tripathi, N., Shukla, A. K., Sahu, R., Thampan, N. M.,
636 Gaddamidi, S., Dixit, K., Ganguly, D., Tiwari, S., Srivastava, A. K., Sahu, L., Rastogi, N., Gargava, P., &
637 Tripathi, S. N. (2022). Effect of Biomass Burning on PM_{2.5} Composition and Secondary Aerosol Formation
638 During Post-Monsoon and Winter Haze Episodes in Delhi. *Journal of Geophysical Research: Atmospheres*,
639 127(1), 1–21. <https://doi.org/10.1029/2021JD035232>

640 Lalchandani, Vipul, Kumar, V., Tobler, A., M. Thampan, N., Mishra, S., Slowik, J. G., Bhattu, D., Rai, P., Satish,
641 R., Ganguly, D., Tiwari, S., Rastogi, N., Tiwari, S., Močnik, G., Prévôt, A. S. H., & Tripathi, S. N. (2021).
642 Real-time characterization and source apportionment of fine particulate matter in the Delhi megacity area
643 during late winter. *Science of the Total Environment*, 770. <https://doi.org/10.1016/j.scitotenv.2021.145324>

644 Lipfert, F. W. (1994). Filter artifacts associated with particulate measurements: Recent evidence and effects on
645 statistical relationships. *Atmospheric Environment*, 28(20), 3233–3249. <https://doi.org/10.1016/1352->
646 2310(94)00167-J

647 Makkonen, U., Virkkula, A., Mäntykenttä, J., Hakola, H., Keronen, P., Vakkari, V., & Aalto, P. P. (2012). Semi-
648 continuous gas and inorganic aerosol measurements at a Finnish urban site: Comparisons with filters, nitrogen
649 in aerosol and gas phases, and aerosol acidity. *Atmospheric Chemistry and Physics*, 12(12), 5617–5631.
650 <https://doi.org/10.5194/acp-12-5617-2012>

651 Malaguti, A., Mircea, M., La Torretta, T. M. G., Telloli, C., Petralia, E., Stracquadanio, M., & Berico, M. (2015).
652 Comparison of online and offline methods for measuring fine secondary inorganic ions and carbonaceous
653 aerosols in the central mediterranean area. *Aerosol and Air Quality Research*, 15(7), 2641–2653.
654 <https://doi.org/10.4209/aaqr.2015.04.0240>

655 Manchanda, C., Kumar, M., Singh, V., Faisal, M., Hazarika, N., Shukla, A., Lalchandani, V., Goel, V., Thampan,
656 N., Ganguly, D., & Tripathi, S. N. (2021). Variation in chemical composition and sources of PM_{2.5} during the
657 COVID-19 lockdown in Delhi. *Environment International*, 153(December 2020), 106541.
658 <https://doi.org/10.1016/j.envint.2021.106541>

659 Minguillón, M. C., Querol, X., Baltensperger, U., & Prévôt, A. S. H. (2012). Fine and coarse PM composition and
660 sources in rural and urban sites in Switzerland: Local or regional pollution? *Science of the Total Environment*,

661 427–428, 191–202. <https://doi.org/10.1016/j.scitotenv.2012.04.030>

662 Nagar, P. K., Singh, D., Sharma, M., Kumar, A., Aneja, V. P., George, M. P., Agarwal, N., & Shukla, S. P. (2017).
663 Characterization of PM_{2.5} in Delhi: role and impact of secondary aerosol, burning of biomass, and municipal
664 solid waste and crustal matter. *Environmental Science and Pollution Research*, 24(32), 25179–25189.
665 <https://doi.org/10.1007/s11356-017-0171-3>

666 Nault, B. A., Campuzano-Jost, P., Day, D. A., Guo, H., Jo, D. S., Handschy, A. V., Pagonis, D., Schroder, J. C.,
667 Schueneman, M. K., Cubison, M. J., Dibb, J. E., Hodzic, A., Hu, W., Palm, B. B., & Jimenez, J. L. (2020).
668 Interferences with aerosol acidity quantification due to gas-phase ammonia uptake onto acidic sulfate filter
669 samples. *Atmospheric Measurement Techniques*, 13(11), 6193–6213. [https://doi.org/10.5194/amt-13-6193-](https://doi.org/10.5194/amt-13-6193-2020)
670 2020

671 Nicolás, J. F., Galindo, N., Yubero, E., Pastor, C., Esclapez, R., & Crespo, J. (2009). Aerosol inorganic ions in a
672 semiarid region on the Southeastern Spanish mediterranean coast. *Water, Air, and Soil Pollution*, 201(1–4),
673 149–159. <https://doi.org/10.1007/s11270-008-9934-2>

674 Nie, W., Wang, T., Gao, X., Pathak, R. K., Wang, X., Gao, R., Zhang, Q., Yang, L., & Wang, W. (2010).
675 Comparison among filter-based, impactor-based and continuous techniques for measuring atmospheric fine
676 sulfate and nitrate. *Atmospheric Environment*, 44(35), 4396–4403.
677 <https://doi.org/10.1016/j.atmosenv.2010.07.047>

678 Pakkanen, T. A., & Hillamo, R. E. (2002). Comparison of sampling artifacts and ion balances for a Berner low-
679 pressure impactor and a virtual impactor. *Boreal Environment Research*, 7(2), 129–140.

680 Pandolfi, M., Querol, X., Alastuey, A., Jimenez, J. L., Jorba, O., Day, D., Ortega, A., Cubison, M. J., Comerón, A.,
681 Sicard, M., Mohr, C., Prévôt, A. S. H., Minguillón, M. C., Pey, J., Baldasano, J. M., Burkhardt, J. F., Seco, R.,
682 Peñuelas, J., Van Drooge, B. L., ... Szidat, S. (2014). Effects of sources and meteorology on particulate matter
683 in the Western Mediterranean Basin: An overview of the DAURE campaign. *Journal of Geophysical*
684 *Research*, 119(8), 4978–5010. <https://doi.org/10.1002/2013JD021079>

685 Pant, P., Shukla, A., Kohl, S. D., Chow, J. C., Watson, J. G., & Harrison, R. M. (2015). Characterization of ambient
686 PM_{2.5} at a pollution hotspot in New Delhi, India and inference of sources. *Atmospheric Environment*, 109,
687 178–189. <https://doi.org/10.1016/j.atmosenv.2015.02.074>

688 Panteliadis, P., Helmink, H. J. P., Koopman, P. C., Hoonhout, M., Jonge, D. De, & Visser, J. H. (2012). *PM 10*
689 *sampling inlets comparison : EPA vs EU. 12341*(1999), 12341.

690 Park, S. S., Cho, S. Y., Jo, M. R., Gong, B. J., Park, J. S., & Lee, S. J. (2014). Field evaluation of a near-real time
691 elemental monitor and identification of element sources observed at an air monitoring supersite in Korea.
692 *Atmospheric Pollution Research*, 5(1), 119–128. <https://doi.org/10.5094/APR.2014.015>

693 Patel, A., Rastogi, N., Gandhi, U., & Khatri, N. (2021). Oxidative potential of atmospheric PM10 at five different
694 sites of Ahmedabad, a big city in Western India. *Environmental Pollution*, 268, 115909.
695 <https://doi.org/10.1016/j.envpol.2020.115909>

696 Pathak, R. K., & Chan, C. K. (2005). Inter-particle and gas-particle interactions in sampling artifacts of PM2.5 in
697 filter-based samplers. *Atmospheric Environment*, 39(9), 1597–1607.
698 <https://doi.org/10.1016/j.atmosenv.2004.10.018>

699 Peck, J., Gonzalez, L. A., Williams, L. R., Xu, W., Croteau, P. L., Timko, M. T., Jayne, J. T., Worsnop, D. R.,
700 Miake-Lye, R. C., & Smith, K. A. (2016). Development of an aerosol mass spectrometer lens system for
701 PM2.5. *Aerosol Science and Technology*, 50(8), 781–789. <https://doi.org/10.1080/02786826.2016.1190444>

702 Pope, C. A., Ezzati, M., & Dockery, D. W. (2009). Fine-Particulate Air Pollution and Life Expectancy in the United
703 States. *New England Journal of Medicine*, 360(4), 376–386. <https://doi.org/10.1056/nejmsa0805646>

704 Querol, X., Pey, J., Minguillón, M. C., Pérez, N., Alastuey, A., Viana, M., Moreno, T., Bernabé, R. M., Blanco, S.,
705 Cárdenas, B., Vega, E., Sosa, G., Escalona, S., Ruiz, H., & Artíñano, B. (2008). PM speciation and sources in
706 Mexico during the MILAGRO-2006 campaign. *Atmospheric Chemistry and Physics*, 8(1), 111–128.
707 <https://doi.org/10.5194/acp-8-111-2008>

708 Rai, P., Furger, M., El Haddad, I., Kumar, V., Wang, L., Singh, A., Dixit, K., Bhattu, D., Petit, J. E., Ganguly, D.,
709 Rastogi, N., Baltensperger, U., Tripathi, S. N., Slowik, J. G., & Prévôt, A. S. H. (2020). Real-time
710 measurement and source apportionment of elements in Delhi's atmosphere. *Science of the Total Environment*,
711 742. <https://doi.org/10.1016/j.scitotenv.2020.140332>

712 Rai, P., Slowik, J. G., Furger, M., El Haddad, I., Visser, S., Tong, Y., Singh, A., Wehrle, G., Kumar, V., Tobler, A.
713 K., Bhattu, D., Wang, L., Ganguly, D., Rastogi, N., Huang, R. J., Necki, J., Cao, J., Tripathi, S. N.,
714 Baltensperger, U., & Prevot, A. S. H. (2021). Highly time-resolved measurements of element concentrations
715 in PM10 and PM2.5: Comparison of Delhi, Beijing, London, and Krakow. *Atmospheric Chemistry and*
716 *Physics*, 21(2), 717–730. <https://doi.org/10.5194/acp-21-717-2021>

717 Rastogi, N., & Sarin, M. M. (2005). Long-term characterization of ionic species in aerosols from urban and high-
718 altitude sites in western India: Role of mineral dust and anthropogenic sources. *Atmospheric Environment*,
719 39(30), 5541–5554. <https://doi.org/10.1016/j.atmosenv.2005.06.011>

720 Rengarajan, R., Sarin, M. M., & Sudheer, A. K. (2007). Carbonaceous and inorganic species in atmospheric aerosols
721 during wintertime over urban and high-altitude sites in North India. *Journal of Geophysical Research*
722 *Atmospheres*, 112(21), 1–16. <https://doi.org/10.1029/2006JD008150>

723 Schaap, M., Spindler, G., Schulz, M., Acker, K., Maenhaut, W., Berner, A., Wieprecht, W., Streit, N., Müller, K.,
724 Brüggemann, E., Chi, X., Putaud, J. P., Hitzenberger, R., Puxbaum, H., Baltensperger, U., & Ten Brink, H.

725 (2004). Artefacts in the sampling of nitrate studied in the “iNTERCOMP” campaigns of EUROTRAC-
726 AEROSOL. *Atmospheric Environment*, 38(38), 6487–6496. <https://doi.org/10.1016/j.atmosenv.2004.08.026>

727 Sharma, D., & Kulshrestha, U. C. (2014). Spatial and temporal patterns of air pollutants in rural and urban areas of
728 India. *Environmental Pollution*, 195(2), 276–281. <https://doi.org/10.1016/j.envpol.2014.08.026>

729 Sharma, S. K., Mandal, T. K., Jain, S., Saraswati, Sharma, A., & Saxena, M. (2016). Source Apportionment of
730 PM_{2.5} in Delhi, India Using PMF Model. *Bulletin of Environmental Contamination and Toxicology*, 97(2),
731 286–293. <https://doi.org/10.1007/s00128-016-1836-1>

732 Shukla, A. K., Lalchandani, V., Bhattu, D., Dave, J. S., Rai, P., Thamban, N. M., Mishra, S., Gaddamidi, S.,
733 Tripathi, N., Vats, P., Rastogi, N., Sahu, L., Ganguly, D., Kumar, M., Singh, V., Gargava, P., & Tripathi, S. N.
734 (2021). Real-time quantification and source apportionment of fine particulate matter including organics and
735 elements in Delhi during summertime. *Atmospheric Environment*, 261(July), 118598.
736 <https://doi.org/10.1016/j.atmosenv.2021.118598>

737 Singh, A., Rastogi, N., Kumar, V., Slowik, J. G., Satish, R., Lalchandani, V., Thamban, N. M., Rai, P., Bhattu, D.,
738 Vats, P., Ganguly, D., Tripathi, S. N., & Prévôt, A. S. H. (2021). Sources and characteristics of light-absorbing
739 fine particulates over Delhi through the synergy of real-time optical and chemical measurements. *Atmospheric*
740 *Environment*, 252(March). <https://doi.org/10.1016/j.atmosenv.2021.118338>

741 Singh, A., Satish, R. V., & Rastogi, N. (2019). Characteristics and sources of fine organic aerosol over a big semi-
742 arid urban city of western India using HR-ToF-AMS. *Atmospheric Environment*, 208(April), 103–112.
743 <https://doi.org/10.1016/j.atmosenv.2019.04.009>

744 Singhai, A., Habib, G., Raman, R. S., & Gupta, T. (2017). Chemical characterization of PM_{1.0} aerosol in Delhi and
745 source apportionment using positive matrix factorization. *Environmental Science and Pollution Research*,
746 24(1), 445–462. <https://doi.org/10.1007/s11356-016-7708-8>

747 Takahama, S., Wittig, A. E., Vayenas, D. V., Davidson, C. I., & Pandis, S. N. (2004). Modeling the diurnal variation
748 of nitrate during the Pittsburgh Air Quality Study. *Journal of Geophysical Research D: Atmospheres*, 109(16).
749 <https://doi.org/10.1029/2003JD004149>

750 Tobler, A., Bhattu, D., Canonaco, F., Lalchandani, V., Shukla, A., Thamban, N. M., Mishra, S., Srivastava, A. K.,
751 Bisht, D. S., Tiwari, S., Singh, S., Močnik, G., Baltensperger, U., Tripathi, S. N., Slowik, J. G., & Prévôt, A.
752 S. H. (2020). Chemical characterization of PM_{2.5} and source apportionment of organic aerosol in New Delhi,
753 India. *Science of the Total Environment*, 745. <https://doi.org/10.1016/j.scitotenv.2020.140924>

754 Tremper, A. H., Font, A., Priestman, M., Hamad, S. H., Chung, T. C., Pribadi, A., Brown, R. J. C., Goddard, S. L.,
755 Grassineau, N., Petterson, K., Kelly, F. J., & Green, D. C. (2018). Field and laboratory evaluation of a high
756 time resolution x-ray fluorescence instrument for determining the elemental composition of ambient aerosols.

757 *Atmospheric Measurement Techniques*, 11(6), 3541–3557. <https://doi.org/10.5194/amt-11-3541-2018>

758 USEPA, & Etv. (2012). *Environmental Technology Verification Report Cooper Environmental Services LLC † Xact*
759 *625 Particulate Metals Monitor. September 2012.* <http://cooperenvironmental.com/>

760 Viana, M., Chi, X., Maenhaut, W., Cafmeyer, J., Querol, X., Alastuey, A., Mikuška, P., & Večeřa, Z. (2006).
761 Influence of sampling artefacts on measured PM, OC, and EC levels in carbonaceous aerosols in an urban
762 area. *Aerosol Science and Technology*, 40(2), 107–117. <https://doi.org/10.1080/02786820500484388>

763 Wang, M., Aaron, C. P., Madrigano, J., Hoffman, E. A., Angelini, E., Yang, J., Laine, A., Vetterli, T. M., Kinney, P.
764 L., Sampson, P. D., Sheppard, L. E., Szpiro, A. A., Adar, S. D., Kirwa, K., Smith, B., Lederer, D. J., Diez-
765 Roux, A. V., Vedal, S., Kaufman, J. D., & Barr, R. G. (2019). Association between long-term exposure to
766 ambient air pollution and change in quantitatively assessed emphysema and lung function. *JAMA - Journal of*
767 *the American Medical Association*, 322(6), 546–556. <https://doi.org/10.1001/jama.2019.10255>

768 Wu, W. S., & Wang, T. (2007). On the performance of a semi-continuous PM_{2.5} sulphate and nitrate instrument
769 under high loadings of particulate and sulphur dioxide. *Atmospheric Environment*, 41(26), 5442–5451.
770 <https://doi.org/10.1016/j.atmosenv.2007.02.025>

771 Zhang, D., Shi, G. Y., Iwasaka, Y., & Hu, M. (2000). Mixture of sulfate and nitrate in coastal atmospheric aerosols:
772 Individual particle studies in Qingdao (36°04'N, 120°21'E), China. *Atmospheric Environment*, 34(17), 2669–
773 2679. [https://doi.org/10.1016/S1352-2310\(00\)00078-9](https://doi.org/10.1016/S1352-2310(00)00078-9)

774 Zhang, X., & Mcmurry, P. H. (1992). EVAPORATIVE LOSSES OF FINE PARTICULATE NITRATES DURING
775 SAMPLING. In *Atmospheric Environment* (Vol. 26, Issue 18).

776